Agricultural and Forest Meteorology 276–277 (2019) 107616

Contents lists available at ScienceDirect

Agricultural and Forest Meteorology

journal homepage: www.elsevier.com/locate/agrformet

Multi-scale temporal variation in methane emission from an alpine peatland on the Eastern Qinghai-Tibetan Plateau and associated environmental controls

Haijun Peng[a,b], Qian Guo[a,b,c], Hanwei Ding[a,b,c], Bing Hong[a,b,d,*], Yongxuan Zhu[a], Yetang Hong[a], Cheng Cai[e], Yu Wang[a], Linggui Yuan[a,b]

[a] State Key Laboratory of Environmental Geochemistry, Institute of Geochemistry, Chinese Academy of Sciences, Guiyang, 550081, China
[b] Bayinbuluk alpine wetland research station, Chinese Flux Observation and Research Network
[c] University of Chinese Academy of Sciences, Beijing, 100049, China
[d] CAS Center for Excellence in Quaternary Science and Global Change , Xi'an, 710061, China
[e] School of Chemical Engineering, Guizhou Institute of Technology, Guiyang, 550055, China

ARTICLE INFO

Keywords:
Methane Emission
Eddy Covariance
Alpine Peatland
Wavelet Analysis
Qinghai-Tibetan Plateau
Temporal Variation

ABSTRACT

Most previous studies on methane (CH_4) emissions from peatlands have focused on the boreal, subarctic, and tropical regions. Little is known about CH_4 emissions from the alpine peatlands that are widely distributed in the eastern Qinghai-Tibetan Plateau (QTP), which are sensitive to climate change and human disturbance. To assess the magnitudes of daily and seasonal variations in CH_4 flux in this area, and to identify the influential environmental factors, an eddy covariance (EC) tower with a LI-7700 open-path CH_4 analyzer was established on Hongyuan Peatland. Total annual CH_4 emission was 46.8 g CH_4 m^{-2} in 2014, with emissions in the non-growing season accounting for 25% of the annual total. From May to September 2014, diurnal variation in CH_4 emissions was observed, with CH_4 fluxes varying between 0.15 and 0.25 μmol m^{-2} s^{-1}. In contrast, during all other periods of 2014, no diurnal variation was observed, and CH_4 flux varied below 0.05 μmol m^{-2} s^{-1}. A clear seasonal pattern in CH_4 exchange with small surges in CH_4 emission appeared in soil thawing and freezing seasons. Wavelet analysis was applied to the continuous CH_4 flux time series to explore temporal variation in ecosystem CH_4 exchange during the growing season. On daily timescales, changes in CH_4 flux are in phase with changes in air temperature, and influenced by friction velocity and vapor pressure deficit (VPD). On weekly-to-monthly timescales, soil temperature can explain most of the variation in CH_4 exchange. Though CH_4 fluxes had no apparent correlation with water table level, fluxes were significantly ($R^2 = 0.86$) correlated with soil temperature measured at -25 cm depth, close to the water table level throughout the growing season, suggesting a synergistic effect of water table level and soil temperature on methane emission. This study highlights the need for continuous eddy covariance measurements and time series analysis approaches to adequately describe temporal variability in ecosystem CH_4 exchange.

1. Introduction

Methane (CH_4) is a powerful, long-lived greenhouse gas (LLGHG) which strongly affects atmospheric chemistry and is responsible for 17% of the radiative forcing caused by LLGHGs. On a centennial time scale, the global warming potential (GWP_{100}) of CH_4 is 28 times greater than that of CO_2 (Stocker et al., 2014). Recent monitoring shows that atmospheric CH_4 concentration reached 1853 ± 2 ppb (parts per billion) in 2016, which is 257% greater than pre-industrial levels(WMO/GAW, 2017). Wetlands are the most abundant natural source for atmospheric CH_4, contributing 30–50% of total global surface CH_4 emissions (Dlugokencky et al., 2011; Fletcher et al., 2004; Kirschke et al., 2013). However, due to a lack of understanding of the controls on CH_4 emission dynamics at the ecosystem scale, high uncertainty remains in current wetland CH_4 budget estimates. Published CH_4 budgets for natural wetlands range from 92–281 Tg yr^{-1} (Fung et al., 1991; Khalil and Rasmussen, 1983; Kirschke et al., 2013; Walter et al., 2001; Zhang et al., 2017). These uncertainties can be attributed to two main factors. First, large discrepancies can develop when comparing bottom-up estimates based on upscaling from field inventories with budgets

* Corresponding author.
E-mail address: hongbing@mail.gyig.ac.cn (B. Hong).

https://doi.org/10.1016/j.agrformet.2019.107616
Received 13 December 2018; Received in revised form 23 May 2019; Accepted 5 June 2019
Available online 14 June 2019
0168-1923/

derived from inverse modeling (Bousquet et al., 2011; Bridgham et al., 2013; Houweling et al., 2017). Second, there are limited data on CH_4 fluxes for many wetlands; thus spatial and temporal heterogeneity in ecosystem CH_4 exchange has not been well characterized (Hendriks et al., 2010; Koebsch et al., 2015; Wei et al., 2015).

Peatlands are one of the most extensive wetland ecosystems globally, and together they release about 30 Tg CH_4 into the atmosphere each year (Frolking et al., 2011). Though they cover only 3% of the Earth's land surface, the global peatlands contain more than 500 Pg of C, which is equivalent to one third of the global soil carbon pool (Gorham, 1991; Turunen et al., 2002; Yu et al., 2010). In recent years, many studies have been carried out worldwide to estimate peatland CH_4 emissions and their dependences on environmental factors (Carroll et al., 2011; Lai et al., 2012; Miao et al., 2012; Rinne et al., 2007). However, most of these studies have focused on peatlands at relatively low elevations. Therefore, further research into alpine peatlands is required to expand our understanding of how these areas contribute to the global CH_4 emission budget and respond to global environmental change. Most of the peatlands on the Qinghai-Tibetan Plateau (QTP) have developed in the Ruoergai Basin (RB), which is located in the eastern QTP. The RB (also known as the Ruoergai Plateau), contains around 4,600 km^2 of peatlands at an average elevation of 3,400 m above sea level (m.a.s.l.), which makes it one of the largest alpine peatlands in the world (Chai, 1981; Chen et al., 2014; Xiang et al., 2009). The environment of the eastern QTP is highly sensitive to rapid global climate change owing to its high altitude and complex topography, as well as its bioclimatic position, which results in influences from the Indian summer monsoon, Eastern Asian summer monsoon, and westerly circulation (Hong et al., 2005; Thomas et al., 2014). In addition, the RB is surrounded by mountains that experience permafrost or seasonal permafrost (Cui et al., 2015; Genxu et al., 2008), which makes the RB peatlands ideal for studying the environmental controls that influence CH_4 fluxes, and evaluating the response of peatlands to global change.

A number of studies into alpine wetland CH_4 exchange have been conducted on the eastern QTP in the past two decades (Chen et al., 2013; Chen et al., 2010; Chen et al., 2008; Deng et al., 2013; Hirota et al., 2004; Jin et al., 1999; Wang et al., 2002; Yang et al., 2014). However, these studies were carried out using low-resolution measurements collected by the traditional static chamber method, and mostly focused on CH_4 exchange during the growing season. As pointed out by Mosier and Bouwman (1990), the installation of the chamber may change temperature and pressure, thus altering the gas diffusion gradient within the soil profile (Koskinen et al., 2014). In contrast, the eddy covariance (EC) method is a non-destructive, micro-meteorological approach for gas flux measurements on ecosystem scales (Baldocchi et al., 2001). With the aid of the newly developed LI-7700 CH_4 analyzer (Detto et al., 2011; McDermitt et al., 2011), EC CH_4 flux measurements have been utilized in a broad range of research, especially in remote sites where grid power is limited. The EC method provides not only a direct signal of land-atmosphere CH_4 exchange but also records continuous CH_4 fluxes which are ideally suited for time series analysis. However, research on the temporal variability of ecosystem CH_4 exchange using time series analysis remains limited. Hatala et al. (2012a) used wavelet analysis to decompose continuous EC CH_4 flux time series, identifying the controls of ecosystem photosynthesis on the diurnal variation pattern of CH_4 flux. With the same technique, Koebsch et al. (2015) revealed the complexity of ecosystem CH_4 exchange, and Cove et al. (2016) showed that ecosystem CH_4 exchange has cross-scale, nonlinear, and asynchronous interactions with various environmental factors. These studies have shown wavelet analysis to be a powerful method that can be used to reveal temporal variability in ecosystem CH_4 exchange and its dependencies on environmental controls. However, studies using time series analysis to investigate the dynamics of alpine peatland CH_4 emissions are still rare.

Like the high-latitude 'Northern Peatlands' (Gorham, 1991), peatlands on the QTP have a long non-growing season and high soil carbon density (Chen et al., 2014; Wang et al., 2015). These conditions allow for detailed studies into alpine wetland ecosystem CH_4 exchange to be carried out, which can provide insight into the dynamics and budgets of high-latitude wetland CH_4 emissions. Based on static chamber measurements in the Huashixia wetlands (35°39′ N, 98°48′ E, 4300–4500 m.a.s.l.), Jin et al. (1999) estimated that the annual CH_4 emission from wetland on the QTP is 0.7–0.9 Tg CH_4 yr^{-1}, and also pointed out wetlands in RB were hotspots of CH_4 emission. Combining EC measurements in the Luanhaizi (37°35′ N, 101°20′ E, 3250 m.a.s.l.) and a sophisticated biogeochemistry model, Jin et al. (2015) estimated wetland on the QTP was a net CH_4 source, emitting 0.95 Tg CH_4 yr^{-1} to the atmosphere. However, the CH_4 emission data used in these studies were limited, with continuous CH_4 flux measurements being needed for a more accurate evaluation of alpine wetland CH_4 emission dynamics and budget. Societal and policy-based motivations for studying CH_4 emissions in the Ruoergai peatlands include the fact that the Ruoergai Plateau is the primary water source to the headstream of the Yellow River, and the fifth largest center of livestock production in China (Xiang et al., 2009). Peatlands in the RB have suffered severe ecosystem degradation since the 1970s, due to poor management practices in the peatlands, such as peat exploitation, livestock over-grazing, and drainage (Chen et al., 2014; Yao et al., 2011). Hence, baseline information on methane fluxes from peatlands in the Ruoergai Plateau is required for insight into how methane fluxes may change if peatlands continue to be degraded to pastures and farmland.

This study presents the results of year-round field CH_4 flux monitoring conducted in an alpine peatland in RB. CH_4 fluxes were measured by the EC system with a LI-7700 CH_4 analyzer. Based on half-hour CH_4 flux time series derived from the EC measurements, the temporal dynamics of ecosystem CH_4 exchange on multiple time scales of hours to months during the growing season were also investigated. The overarching objectives of this study were to (1) investigate the temporal variability in CH_4 fluxes and environmental factors across hourly, daily and seasonal time scales, (2) identify which processes control ecosystem CH_4 exchange at specific time scales and time periods, and (3) evaluate the annual CH_4 budget, and the contribution of the non-growing season CH_4 emissions to the yearly budget.

2. Materials and methods

2.1. Site description

The study was conducted at the Hongyuan Peatland Carbon Flux Monitoring and Research Station of the Institute of Geochemistry, Chinese Academy of Sciences, in Hongyuan County, Sichuan Province, China (32°46′ N, 102°30′ E, 3510 m.a.s.l.). The Hongyuan peatland is part of the Ruoergai wetlands, which developed in the Ruoergai Basin (RB) on the eastern QTP (Fig. 1a). The dominant plant populations in the peatland are *Carex mulieensis* and *Kobresia tibetica*. The climate of this region is characterized by intense solar radiation with long, severe winters and short, cool summers. During the past three decades (1981–2010), the mean annual temperature in Hongyuan was 1.75 °C, with mean monthly air temperature ranging from −9.4 °C in January to 11.2 °C in July. Mean annual precipitation for that period was 746.1 mm, with more than 75% of precipitation occurring during the growing season from May to September (raw data from the Information Center of China Meteorological Administration (http://www.nmic.cn).

The Hongyuan peatland is a typical mountain valley peatland that has developed over the last 12,000 years in a valley located on the south side of the White River (*Hong et al.*, 2003). The accumulation of extensive peat in this region has been aided by the unique climate and topographic conditions in the area. Before installation of the research station, the spatial distribution of the peatland was surveyed using a MALÅ ProEx ground penetrating radar with a 50 MHz RTA antenna (MALÅ Geosciences, Sweden), and a Russian Peat Corer. Results

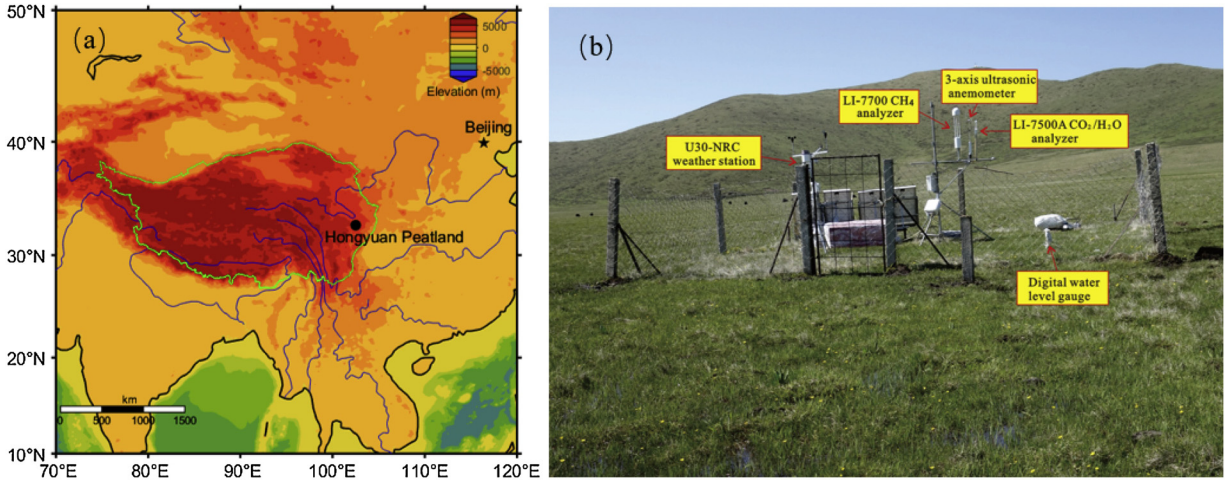

Fig. 1. (a) Geographic location of Hongyuan Peatland (green line represents the boundary of the Qinghai-Tibetan Plateau), terrain data retrieved from the NOAA Data Announcement 88-MGG-02 (https://www.ngdc.noaa.gov/mgg/global/etopo5.HTML) at 7 March 2019; (b) Landscape and instruments installed at the Hongyuan Peatland Carbon Flux Monitoring and Research Station.

showed that the depth of Hongyuan peatland ranges from 0.5 and 6.5 m. A layer of grey-greenish silty sediments lies beneath the peat deposit. The total area of the Hongyuan Peatland was measured to be 1.1 km^2. The EC tower was installed in the center of the peatland, where the terrain is flat, and ideal for micrometeorological flux measurements. The flat area has a diameter of more than 300 m diameters, and the peat depth at the installation site is 6.5 m.

2.2. Eddy Covariance and Meteorological and Soil Measurements

CH_4 flux was measured from 19 November 2013 to 11 May 2015. A total of 25,829 30 min observations were collected. During 21 May–12 June, 4–22 July, and 11–24 December 2014, the EC system stopped recording due to system malfunctions. CH_4 concentration was measured with an open-path CH_4 analyzer (LI-7700, LI-COR Inc., USA). Wind and turbulence were measured with a three-dimensional ultrasonic anemometer (WindMaster Pro, Gill Instruments Limited, UK). Water vapor and carbon dioxide molar densities were measured with an open-path, infrared spectrometer (LI-7500A, LI-COR Inc., USA). The separation of the three sensors was 15 cm, and all sensors were elevated 2.5 m above ground level (Fig. 1b). The prevailing wind direction was from the north. To minimize airflow disturbances, the anemometer was installed with a northward horizontal separation of 10 cm from the CH_4 and CO_2/H_2O sensors. Data from the anemometer, LI-7500A, and LI-7700 were recorded at 10 Hz using a LI-7550 data logger (LI-COR Inc., USA).

To measure the level of the water table, a two m-deep hydrological well was drilled. The walls of the well were supported by a 7.8 cm-diameter perforated PVC pipe. Water table level was measured using a ZKGD3000-M digital water level gauge (Beijing Zhongke Guangda Automation Technology CO., LTD, China). A HOBO U30 weather station was also installed at the study site (Fig. 1b). Soil temperatures were measured at depths of -10, -25, and -40 cm, and air temperature at a height of 2 m, with a 12-Bit Temperature Smart Sensor (S-TMB-M006, Onset Computer Corporation, USA). These observations are reported as ST-10, ST-25, ST-40, and AT200, respectively. Soil water content at -10 cm depth was measured with a 10HS Soil Moisture Smart Sensor (S-SMD-M005, Onset Computer Corporation, USA). Solar radiation was measured using a silicon pyranometer sensor (S-LIB-M003, Onset Computer Corporation, USA), and precipitation was measured with a Rainfall Smart Sensor (S-RGB-M002, Onset Computer Corporation, USA).

2.3. Eddy flux calculation and data quality control

The raw EC data were processed and quality controlled based on the standard methods for EddyPro 5.1.1 (Express mode) (LI-COR Inc., USA), to compute CH_4, *LE* (latent heat) and *H* (sensible heat) fluxes over 30 min intervals (Foken et al., 2005). Spectral attenuations were corrected by the method outlined in Moncrieff et al.(1997). Air density fluctuations were corrected by the Webb-Pearman-Leuning (WPL) correction (Webb et al., 1980). Sonic temperature was corrected for humidity effects (Van Dijk et al., 2004). The methods of Vickers and Mahrt (1997) were used for time lag compensation, detrending, and statistical testing. Footprint was calculated using the method of Kljun et al. (2004). The footprint evaluation indicated that 90% of the fluxes came from within 127 ± 73 m of the eddy tower during the daytime and 184 ± 110 m during the nighttime, which confirmed that the fluxes are representative of the peatland area.

Although high-frequency spikes were removed before calculation of the 30 min averaged flux, spikes still appeared in the time series of 30 min fluxes. Thus, outlier detection was needed to filter out the CH_4 flux spikes. In this study, spikes were detected using an algorithm based on the position of each 30 min flux with respect to the preceding and subsequent fluxes (Papale et al., 2006). In this method, each 30 min CH_4 flux F_i corresponds to a value d_i, which is calculated as:

$$d_i = (F_i - F_{i-1}) - (F_{i+1} - F_i) \quad (1)$$

Accordingly, F_i is flagged as a spike if:

$$d_i < Md - (z \bullet \mathrm{MAD}/0.6745) \quad (2)$$

or

$$d_i > Md + (z \bullet \mathrm{MAD}/0.6745) \quad (3)$$

where

$$\mathrm{MAD} = \mathrm{median}(|d_i - Md|) \quad (4)$$

and *Md* is the median of the differences; *z* is a threshold value, which equals 7 in this study. Additionally, all of the fluxes that were measured during calm climate conditions, with a friction velocity $u^* < 0.1$ m s^{-1}, were grouped for further analysis (Alberto et al., 2014).

2.4. Gap filling

To date, no standard method has been developed to gap-fill the missing 30 min CH_4 fluxes. Previous studies have variously applied the Marginal Distribution Sampling (MDS) method (Alberto et al., 2014),

the Look-Up Table (LUT) method (Meijide et al., 2011) and the Artificial Neural Network (ANN) technique (Hatala et al., 2012a). Rinne et al. (2007) used the peat temperature at a depth of 35 cm and the depth of the water table as drivers to fit CH_4 emission trends and fill the flux gaps. In the present study, the variation in soil water content at -10 cm depth showed a greater correlation with CH_4 fluxes than water table level. Adopting a similar approach in the study of Rinne et al. (2007), the missing 30 min CH_4 fluxes were gap-filled using ST-25 and soil moisture measured at a depth of 10 cm as meteorological drivers. Linear regression shows 86% of the variations in CH_4 fluxes can be accounted for using this method.

2.5. Wavelet analysis

The spectral characteristics of CH_4 fluxes and its correlation with the spectra of environmental factors were examined using the continuous wavelet transform (CWT) with the Morlet wavelet (Torrence and Compo, 1998). Continuous wavelets are robust to noise, which makes the Morlet wavelet a more powerful tool for analyzing time series with nonstationary than Fourier analysis (Daubechies, 1990; Hatala et al., 2012a; Katul et al., 2001; Torrence and Compo, 1998). The Morlet wavelet has a real and an imaginary part, which facilitates the analysis of amplitude and phase respectively (Cazelles et al., 2008; Grinsted et al., 2004). In order to avoid spurious correlations between CH_4 flux and environmental factors, missing flux, friction velocity (u^*), and VPD values were gap filled with median values before and after the gap. There were no gaps in the temperature and water table level series. Wavelet coherence analysis was used to investigate the correlation between CH_4 fluxes and environmental factors, i.e., air temperature, soil temperature at different depth, u^*, VPD, water table level, and soil temperature gradient in the time-frequency domain. The method of Koebsch et al. (2015) was employed to rate the correlation between CH_4 fluxes and the measured environmental variables, using the phase angle calculated from the time shift between two oscillations. All wavelet analyses were performed in MATLAB (R2016a, MathWorks Inc., USA). The spectral characteristics of CH_4 fluxes only showed clear diurnal variation patterns from May to September, thus the spectral characteristics of CH_4 fluxes and their correlation with the spectral characteristics of environmental factors were only examined during this period.

3. Results

3.1. Environmental conditions

Over the study period, the site was characterized by strong variations in solar radiation, air temperature, and precipitation, with most of the annual precipitation occurring during the growing season while the temperature was high and sunshine was abundant (Fig. 2b, d, f). This climate pattern is conducive to plant growth and plant residue accumulation which is beneficial for the development of peat enriched wetland. Total annual solar radiation in 2014 was 1690 kW m^{-2}, with daily mean solar radiation staying above 200 w m^{-2} h^{-1} throughout most of the growing season (Fig. 2d). The mean annual air temperature and total precipitation in 2014 were 2.8 °C and 795 mm, respectively. The highest daily mean temperature of 15.8 °C and the lowest temperature of −15.6 °C were observed in August and January, respectively (Fig. 2b). Most precipitation occurred in the growing season, with the highest rainfall occurring in September (Fig. 2c). Soil moisture at a depth of 10 cm is influenced by both soil temperature and precipitation (Fig. 2c, e, f).

In order to determine the relations between CH_4 fluxes and climate conditions, the CH_4 fluxes were divided into four time periods: (1) growing season, ranging from the first of seven consecutive days with average daily air temperature above 5 °C to the first of seven consecutive days with average daily air temperature below 5 °C; (2) soil freezing, ranging from the end of the growing season to the first of two consecutive days with an average daily soil temperature below 0 °C at -10 cm depth; (3) winter, starting at the end of the soil freezing period and ending when the soil temperature at -10 cm depth exceeds 0 °C; (4) soil thawing, incorporating the time period between winter and the growing season (Aurela et al., 2002; Lund et al., 2010; Song et al., 2015). Nongrowing season includes soil freezing, winter and soil thawing periods (Table 1).

3.2. Seasonal variations in CH_4 fluxes

Across the periods 21 May–12 June, 4–22 July, and 11–24 December 2014, the EC system was suspended due to a series of system malfunctions. 41% of all the measurements were filtered out due to quality control and system malfunctions, but the remaining 59% covered the full spectrum of temperature and precipitation intensities (Fig. 2). Thus, the remaining data was used for gap-filling and further analysis. The gap-filled data showed that the Hongyuan peatland acted as a source of methane throughout the entire measurement period. CH_4 fluxes showed typical seasonal patterns with the highest fluxes occurring in July and August, and the lowest fluxes occurring in April, which is in accordance with the variations in air temperature and soil temperatures (Fig. 2). The half-hourly CH_4 fluxes showed a relatively large variation, including some negative values. These negative fluxes were mainly recorded during the non-growing season (Fig. 2a), and appeared to be caused by relatively large random uncertainty associated with a single flux value when measuring low fluxes. In general, the fluxes varied between 0 and 0.05 μmol m^{-2} s^{-1} during the non-growing season and between 0.15 and 0.25 μmol m^{-2} s^{-1} during the growing season. From late November 2013 to late April 2014, the daily averaged CH_4 fluxes followed a continuous decreasing trend. No significant increases in CH_4 flux were observed during soil freezing or soil thawing. In the soil thawing period, daily mean CH_4 flux was below 0.05 μmol m^{-2} s^{-1}. In the soil freezing period, daily mean CH_4 flux varied between 0.02 to 0.14 μmol m^{-2} s^{-1}. During the growing season, fluxes remained around 0.15–0.25 μmol m^{-2} s^{-1}, but emissions rapidly decreased during the soil freezing period. During this relatively short period, the methane flux dropped from more than 0.2 μmol m^{-2} s^{-1} to less than 0.05 μmol m^{-2} s^{-1}, before a continuously declining wintertime trend, similar to that recorded across November 2013–April 2014, reappeared from late November 2014 to late April 2015 (Fig. 2a).

3.3. Diurnal variations in CH_4 flux

A significant diurnal pattern in CH_4 flux was observed from May to September 2014, with a peak value occurring at around 16:30 (local time, UTC + 8) (Fig. 3a). However, no clear diurnal cycle was observed in the remaining days of 2014, during which CH_4 emissions were about 4–5 times lower than that in the growing season (Fig. 3b). During the growing season, CH_4 emissions started to increase at around 08:00, reached a peak of (mean ± standard error) 0.185 ± 0.005 μmol CH_4 m^{-2} s^{-1} at 16:30, and then decreased to less than 0.17 μmol CH_4 m^{-2} s^{-1} after 20:00. In contrast, during the non-growing season, CH_4 fluxes varied at levels lower than 0.05 μmol m^{-2} s^{-1}, and showed unstable variations during the night. Clear diurnal variation patterns were also observed in AT2 (Fig. 3d), ST-10 cm (Fig. 3h), solar radiation (Fig. 3c), friction velocity (Fig. 3g), Vapor Pressure Deficit (VPD) (Fig. 3i), wind speed (Fig. 3o), and the temperature gradients (Fig. 3b, f, j, k, m, n). There are no diurnal patterns in ST-25 and ST-40. The peak in CH_4 fluxes is synchronized with the temperature gradients of ST-25 to ST-10 and ST-40 to ST-10. The peak in solar radiation precedes the peak in friction velocity, which is followed by peaks in air temperature, then VPD, then wind speed, and finally ST-10. However, these diurnal variation patterns were calculated from seasonal time scale averages, and therefore do not represent the real-time fluctuations in those variables. Thus, wavelet analysis was used to reveal the shorter timescale

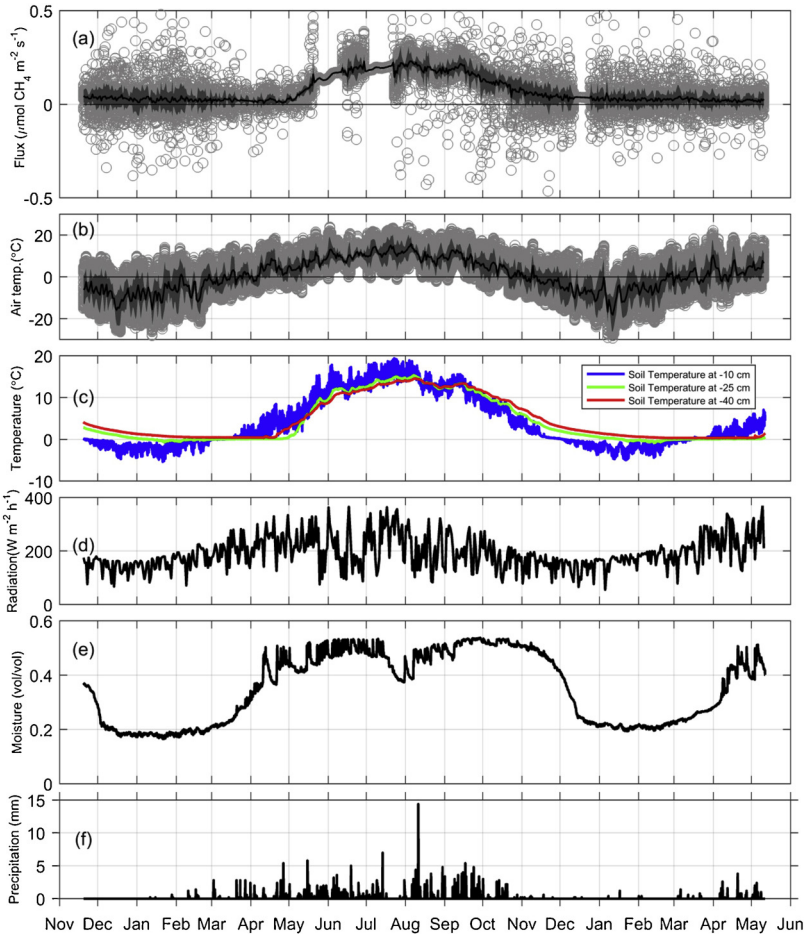

Fig. 2. Time series of CH_4 fluxes and environmental variables: Seasonal dynamics of (a) CH_4 fluxes (the grey circles stand for half-hour fluxes, the black line denotes daily mean fluxes, and the shaded area shows standard deviation for each half-hour interval; (b) air temperature at 2 m above the ground (the grey circles represent half-hourly observations, the black line represents daily means and the shaded area denotes standard deviation for each half-hour interval); (c) soil temperature at 10 cm (blue line), 25 cm (green line), and 40 cm (red line) below the ground; (d) daily mean solar radiation;(e) half-hourly soil moisture at -10 cm depth; (f) half-hourly precipitation.

Table 1
Total CH_4 flux (g CH_4 m^{-2}), number of days recorded, percentage contributions to annual emission, Q_{10} value, correlation coefficients (exponential correlations with soil temperature at 25 cm depth) and mean soil temperatures (°C) at 25 cm depth throughout 2014. Values for the non-growing season are broken down into their component parts. Q_{10} and R^2 were calculated using daily mean gap-filled fluxes; DOY = days of year.

Period	CH_4 Fluxes	Time (DOY)	Contributions (%)	Q_{10}	R^2	Soil Temperature
Growing season	34.89	127-273	74.55	2.93	0.89	11.97
Nongrowing	11.91	1-126 and 274-365	25.45	6.55	0.72	1.87
Soil freezing	6.63	274-336	14.17	4.54	0.83	5.87
Winter	3.46	1-64 and 337-365	7.39	17.15	0.17	0.27
Soil thawing	1.82	65-126	3.89	16.12	0.06	0.21
Total	46.8	1-365	100	5.13	0.91	5.93

variations in ecosystem CH_4 exchange and environmental variables.

3.4. Variations and correlations in the time-frequency domain

The spectral energy peak at the daily scale was clear for CH_4 fluxes, ST-25, friction velocity, VPD, and water table level (Fig. 4). However, the spectral energy peak of water table level on the daily time scale was much lower than the other variables. No common spectral features were observed between CH_4 fluxes and friction velocity, in contrast to the findings of Franz et al. (2016). Plotting the local CH_4 wavelet power spectra in the time-frequency domain revealed additional shorter periods of high variation in ecosystem CH_4 exchange that occurred across time scales of 28–30 days (Fig. 5a). Furthermore, the diurnal variation in ecosystem CH_4 exchange was not consistent throughout the growing season, but limited to periods from mid-May to June, late July to early August, mid-August and late September (Fig. 5a). Variation in CH_4 flux on a daily scale only occurred during short, isolated periods (Fig. 5a).

Patterns of correlation between ecosystem CH_4 exchange and AT200, ST-10, ST-25, and ST-40 were all similar in the time-frequency domain were all similar. However, the phase shift patterns of these variables were different, especially on smaller time scales (Fig. 5b–e). All temperature variables exhibited significant correlation with CH_4 flux on a daily time scale, but only AT200 was in phase with the fluctuations in CH_4 exchanges. The temperature variables also exhibited significant correlation with CH_4 flux and were in phase with the fluctuations in CH_4 exchange on longer time scales. Significant correlations between ecosystem CH_4 exchange and friction velocity and VPD were observed in the two periods that flux data were missing due to instrumental malfunction (Fig. 5f, g). However, these high correlations were caused by the fact that the missing data were gap-filled using the same algorithm. Besides these two periods, CH_4 fluxes only showed significant correlations with friction velocity and VPD on short timescales: VPD was only in phase with CH_4 fluxes on a few short stages, and friction velocity was not in phase with ecosystem CH_4 exchange. The variations in water table level and the temperature gradient were also correlated with CH_4 flux on shorter and longer timescales, but the

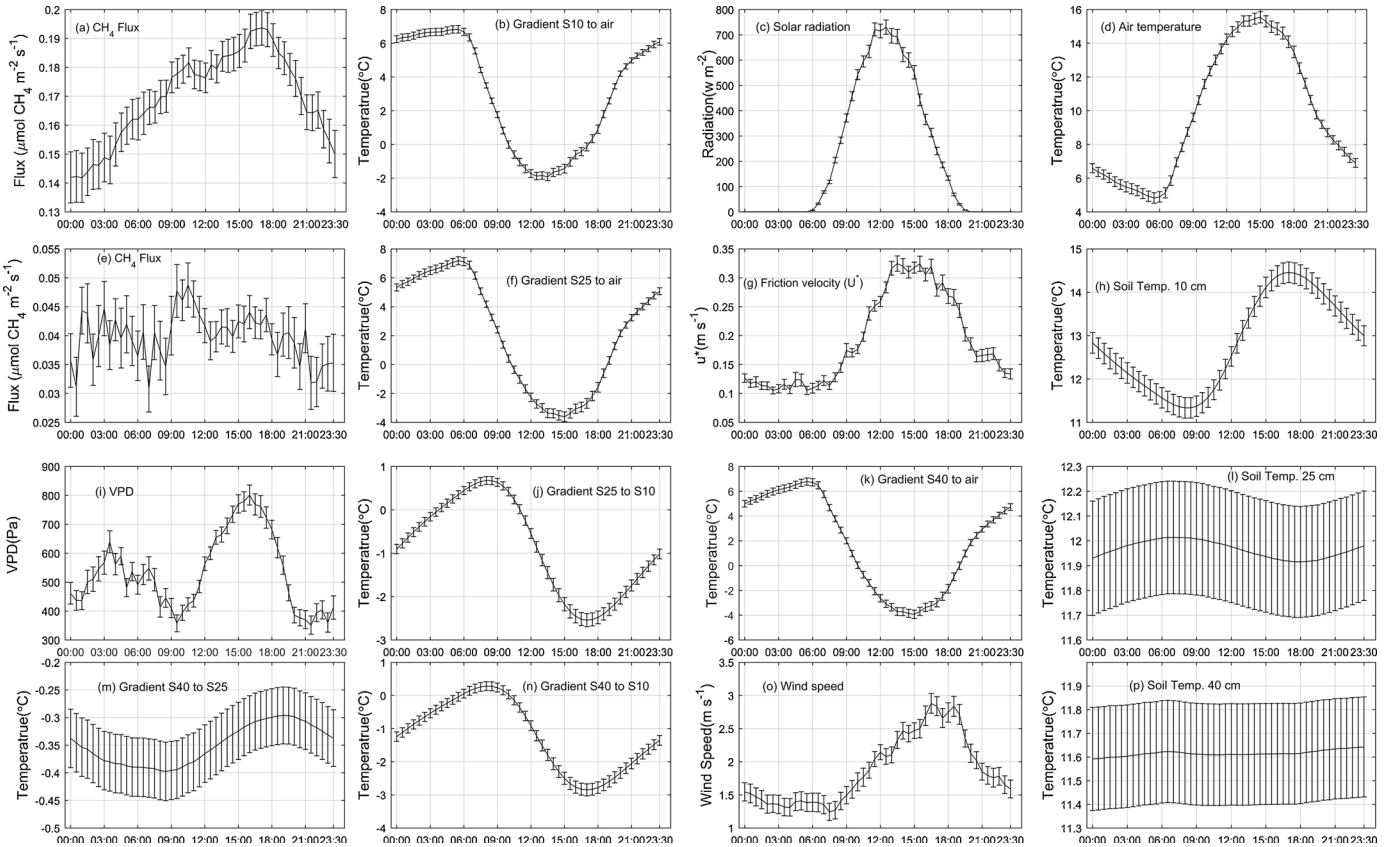

Fig. 3. Average diurnal variations during the growing season (with the exception of part (e)): (a) methane flux; (b) temperature gradient derived from the difference between ST-10 and AT200; (c) solar radiation; (d) air temperature measured at 2 m above the ground (AT200); (e) CH_4 flux in the non-growing season; (f) temperature gradient derived from the difference between ST-25 and AT200; (g) friction velocity; (h) soil temperature at 10 cm depth (ST-10); (i) Vapor Pressure Deficit (VPD); (j) temperature gradient derived from the difference between ST-25 and ST-10; (k) temperature gradient derived from the difference between ST-40 and AT200, (l) soil temperature at 25 cm depth (ST-25); (m) temperature gradient derived from the difference between ST-40 and ST-25; (n) temperature gradient derived from the difference between ST-40 and ST-10; (o) wind speed; (p) soil temperature at 40 cm depth (ST-40). Growing season represents the period from May 1 to September 30; non-growing season represents the remainder of 2014. In temperature gradient plots (b), (f), (j), (k), (m) and (n), positive gradients indicate a density stratification of the soil column whereas negative gradients represent periods of convective mixing. Error bars in all plots denote the standard errors (the number of observations was 212 for the figure (e) and 153 for the rest figures). The time axis in all plots records local time (UTC + 8).

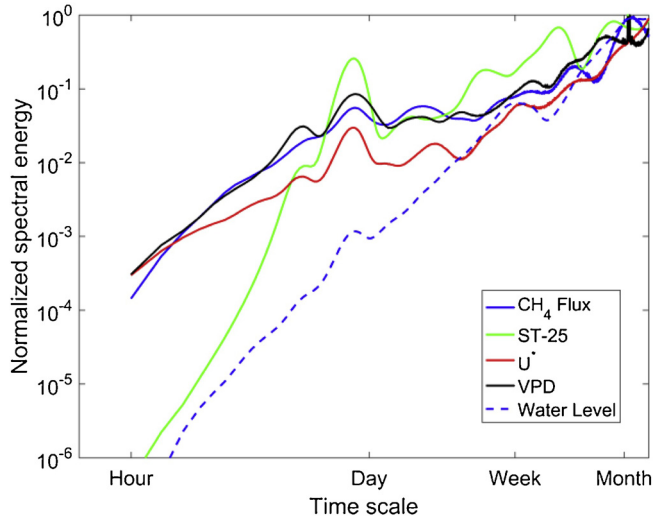

Fig. 4. Normalized global wavelet energy spectra of ecosystem exchange of CH_4 and certain environmental variables. U^* stands for friction velocity, ST-25 is soil temperature measured at 25 cm below the ground, and VPD is vapor pressure deficit.

correlations were not in phase (Fig. 5h, i).

4. Discussion

4.1. Diurnal variations in ecosystem CH_4 exchange

Diurnal variation in CH_4 flux often exhibits different patterns and magnitudes due to differences in wetland types, plant communities, and environmental conditions. Clear diurnal variation patterns have been noted in some previous studies (Alberto et al., 2014; Hatala et al., 2012b; Long et al., 2010; Song et al., 2015); in contrast, other studies have reported that no distinct diurnal pattern was observed during their monitoring (Heyer et al., 2002; Rinne et al., 2007). It should be noted that the diurnal variations observed in previous studies are not consistent with each other. Specifically, discrepancies existed in their variation patterns and when the peak values appeared. In this study, through wavelet analysis, a clear diurnal variation pattern was found to exist only during the growing season (Fig. 5a). This observation implies that the diurnal variation pattern is likely to be caused by changes in vegetation activity. This pattern is in accordance with studies which have reported that clear diurnal patterns in CH_4 flux only appeared when rice is being grown in paddy fields (Alberto et al., 2014; Meijide et al., 2011; Tseng et al., 2010). However, the mechanism of how vegetation activity induces diurnal CH_4 flux peaks still needs to be clarified. Additionally, the growing season diurnal variation pattern

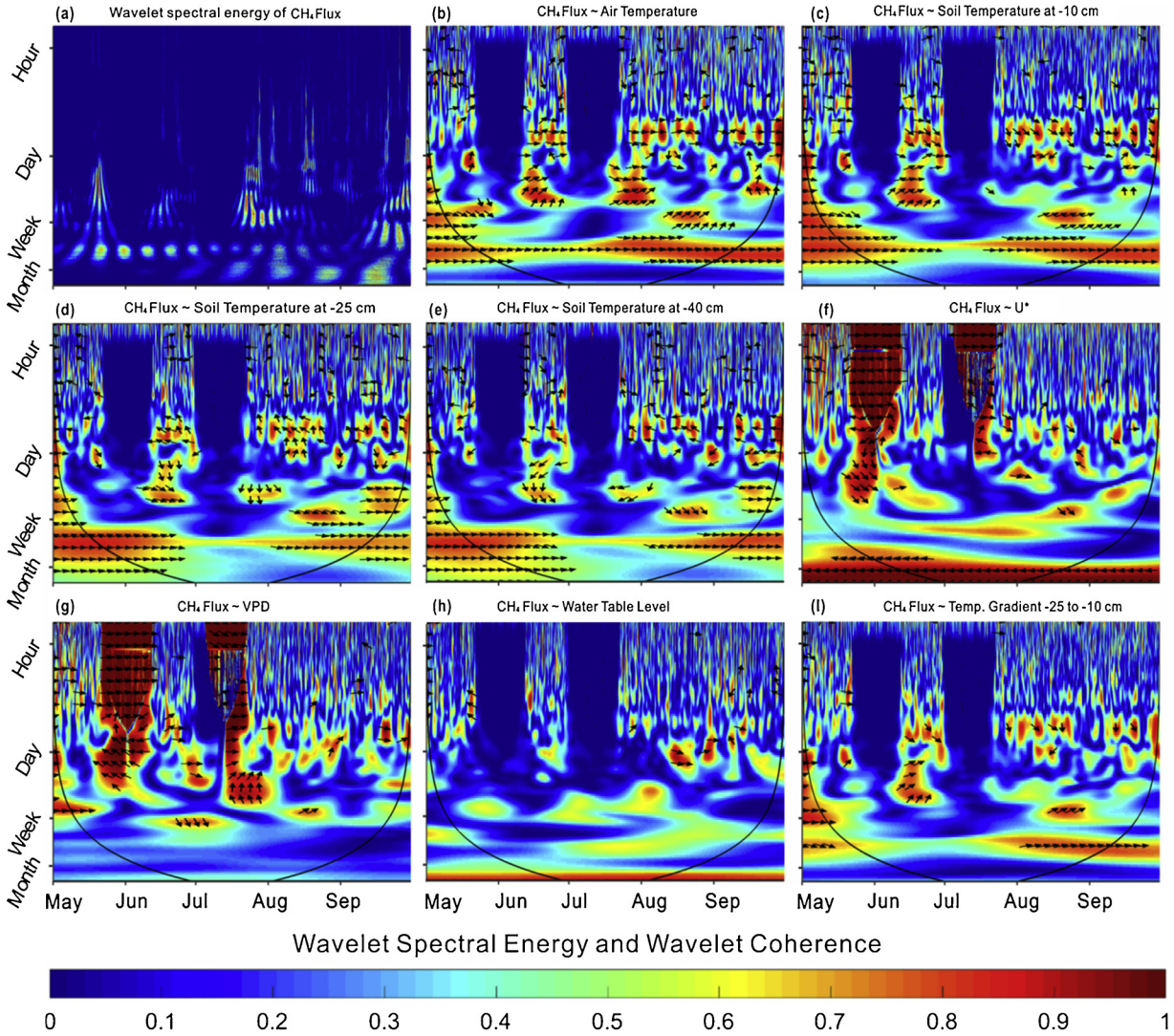

Fig. 5. (a) Wavelet spectral energy of ecosystem CH_4 exchange. The rest of the figure shows wavelet coherence between ecosystem CH_4 exchange and (b) air temperature; (c) ST-10; (d) ST-25; (e) ST-40; (f) friction velocity; (g) VPD; (h) water table level; (i) temperature gradient between ST-25 and ST-10. Red color indicates high correlation strength between CH_4 exchange and a variable for the given time scale. The direction of the black arrows indicates the phase shift between ecosystem CH_4 exchange and the associated variable (right: CH_4 exchange and variable are in phase, which means the series are perfectly correlated; up: CH_4 exchange leads variable by $\pi/2$; left: CH_4 exchange and variable are out of phase, down: CH_4 exchange lags variable by $\pi/2$). The black line represents the cone of influence (Torrence and Compo, 1998), beyond which edge effects are abundant, and results should be interpreted with caution.

showed that daytime CH_4 fluxes were higher than night-time CH_4 fluxes (Fig. 3a), which suggests that estimating annual CH_4 emission by using only daytime CH_4 fluxes may be problematic.

Growing season diurnal variation in CH_4 flux and AT200 displayed single peaks with peak values appearing at 16:30 and 14:00, respectively (Fig. 3a, d), while ST-10 and ST-25 showed sinusoidal patterns (Fig. 3h, l). Neither the variations in air temperature or soil temperature at depths of 10 and 25 cm match the variation in CH_4 flux uniformly. Thus, the environmental variable responsible for the diurnal changes in CH_4 fluxes in the growing season remains unclear. Two possible explanations can be proposed for the observed variability. On one hand, an increase in CH_4 production activity may have caused the diurnal peak in CH_4 fluxes. Methane emission consists of three main phases: methanogenesis, methane oxidation and methane transportation (Bridgham et al., 2013; Conrad, 2005). Methanogenic activities are mainly controlled by temperature and substrate supply (Hendriks et al., 2010; Yvon-Durocher et al., 2014). In the course of one day, ST-25, ST-40, and water table tended to remain relatively stable (Fig. 3l, p, and Fig. 7a), meaning a stable environment for methanogenesis was maintained. However, plants in the peatland, mainly *Carex mulieensis* and *Kobresia tibetica*, usually have long roots that can reach the region below the water table (Hirota et al., 2004). It has been noted that root exudates can provide food to methanogens and stimulate methanogenesis, thus increasing CH_4 production (Hatala et al., 2012a; Vargas and Allen, 2008; Yuan et al., 2012). This process has been observed in the studies of Koebsch et al. (2015) and Hatala et al. (2012a), who showed, through wavelet analysis, that the diurnal variation in ecosystem CH_4 exchange was preceded by a diurnal peak in ecosystem photosynthesis. On the other hand, methane transportation rate can be influenced by a diffusion gradient, and therefore this may have caused the diurnal peak. Since the water table was below a depth of -20 cm throughout most of the growing season (Fig. 7a), it can be deduced that most of the emitted CH_4 came from below this depth during the growing season. Therefore, heat conduction from below to above this depth can be used as an indicator of the diffusion rate. It has been noted that the transportation of CH_4 from water to the soil column and the atmosphere may be driven by the diffusion rate, which is controlled by the temperature gradient between water and the upper soil column (Shoemaker et al., 2012). Thus in the study of Koebsch et al. (2015), temperature gradient was used to represent the convective mixing ratio

of the water column. In this study, the peak in the temperature gradients from ST-25 to ST-10 and S-40 to ST-10 matched the peak in CH_4 flux. This observation illustrates that the diurnal peak in CH_4 flux was also influenced by transportation rate in the soil column. However, direct measurements of CH_4 flux within the soil column, especially CH_4 exchange rate between the water table-air interface, would be needed to validate this explanation.

4.2. Seasonal variations in ecosystem CH_4 exchange

The annual CH_4 emissions of Hongyuan peatland totaled 46.8 g CH_4 m^{-2} in 2014, during which 75% of emissions were released during the growing season. The emissions during the non-growing season were 11.91 g CH_4 m^{-2}, which accounts for 25% of the annual sum (Table 1), indicating that the flux in the non-growing season is non-negligible (Merbold et al., 2013; Wei et al., 2015; Zhu et al., 2011). Due to instrumental and climate condition limitations, CH_4 emissions in the non-growing season have not been fully quantified in previous studies (Chen et al., 2013; Jin et al., 1999; Wang et al., 2002). Considering the total intact peatland area in RB is 3,179 km^2 (Chen et al., 2014), the CH_4 emissions from the RB peatlands are estimated to total around 0.15 Tg CH_4 yr^{-1}, which represents 16% of all QTP wetland emissions (Jin et al., 2015). The temperature sensitivity (Q_{10}) of CH_4 flux (i.e. the increase factor in the rate of CH_4 flux when soil temperature is increased by 10 °C) (Schipper et al., 2014; Song et al., 2015; Ye et al., 2014) was 5.13 in 2014. The Q_{10} for CH_4 flux during the non-growing season and growing season were 6.55 and 2.93, respectively, indicating that CH_4 emission in the non-growing season is more sensitive to warming than in the growing season. Though the Q_{10} values in winter and soil thawing season were much higher than other seasons (Table 1), the exponential correlations between CH_4 flux and temperature were very weak (Table 1). Thus, the Q_{10} value was not used to investigate temperature sensitivity in these two periods.

During the onset of soil thawing, no large surges in CH_4 flux were observed, in contrast to the studies of Hargreaves et al. (2001) and Song et al. (2015). However, small peaks in CH_4 flux were detected in mid-April 2014 and mid-April 2015. Peaks were also recorded in AT200 and ST-10 at the same time (Fig. 2a–c). During these two periods, most of the CH_4 fluxes were measured rather than gap-filled, and the variations in ST-25 were stable. Since the missing data was gap-filled using ST-25 as a meteorological driver, the possibility that these two peaks were caused by gap-filling can be excluded. The CH_4 flux peaks observed in the soil thawing season may be attributable to the release of CH_4 that was stored in soil pores and water (Hargreaves et al., 2001; Rinne et al., 2007), or the thawing process may have accelerated the activity of methanogens (Dörsch et al., 2004). During the onset of soil freezing, the data of this study show a peak in CH_4 flux in late October (Fig. 2a), which varied in conjunction with increases and decreases in AT200 and ST-10. This pattern is similar to results reported in Mastepanov et al. (2008), but the variation in magnitude is smaller. In the present study, AT200 and ST-10 were above 0 °C. Hence this peak is more likely caused by a rise in AT200 and ST-10, rather than a rise in CH_4 gas pressure as gas escapes to the frozen active layer from the permafrost table (Mastepanov et al., 2008).

The annual CH_4 emission of Hongyuan peatland is equivalent to 35.1 g C-CH_4 m^{-2}. This value is 28% to 43% larger than the values that Song et al. (2015) observed at Luanhaizi. The mean annual temperature and annual precipitation of Luanhaizi were reported as -1.1 °C and 490 mm by Song et al. (2015), values that are 2.85 °C and 256.1 mm lower than that of Hongyuan Peatland, respectively. Since methane emission is positively correlated with temperature (Cui et al., 2015; Yvon-Durocher et al., 2014), it is reasonable that peatland CH_4 emission from Luanhaizi is observed to be lower than that from Hongyuan. As pointed out by Jin et al. (2015), spatial heterogeneity is the main factor limiting the accurate estimation of CH_4 emission from wetland on the QTP. The findings of this study have implications for the evaluation of wetland CH_4 emissions from the QTP. First, daily and seasonal patterns in CH_4 flux revealed that annual CH_4 fluxes could be overestimated if only daytime and/or growing season flux data are considered, because large diurnal and seasonal variations occur in the region. In particular, the data of this study show that CH_4 emission during the non-growing season is substantial, and should be included in flux estimations. Second, comparing the results of this study with the measurements gathered in Luanhaizi, confirms that spatial heterogeneity does exist in alpine wetland CH_4 emission. This result implies it may be problematic to evaluate overall QTP CH_4 emissions by using field observations with limited coverage. Thus, continued field monitoring in other areas of the QTP wetland is essential for accurate CH_4 emission evaluation.

4.3. Effects of temperature on ecosystem CH_4 exchange

Methanogenesis is enzymatically mediated and is carried out by strictly anaerobic archaea (Thauer et al., 2008). It has been pointed out that methane is produced by the anaerobic decomposition of organic matter in the soil, especially root organic carbon (ROC), such as that in root exudates (Yuan et al., 2012). The resultant CH_4 is released into the atmosphere from the subsoil, mainly through soil-floodwater interface diffusion (Heyer et al., 2002), gas bubble ebullition (Tokida et al., 2007), and aerenchyma transportation (Morrissey et al., 1993; Thomas et al., 1996). In the course of the emission process, a certain amount of CH_4 can be oxidized by methanotrophic bacteria during diffusion through the rhizosphere and soil layer, and it can also be oxidized through specific chemical reactions in the atmosphere (Conrad, 2005; Crill et al., 1994). It has been shown that methane production, oxidation, and emission processes are all dominantly driven by temperature variations (Yvon-Durocher et al., 2014). However, the dependence of CH_4 fluxes on different temperature parameters (such as air temperature, soil temperature measured at different depths, and water temperature) remains to be tested.

Measured CH_4 flux and air and soil temperatures were used to examine the effect of soil temperature at different depths, and air temperature, on variations in CH_4 flux. The results from this analysis indicate that AT200, ST-10, ST-25, and ST-40 can explain 48%, 80%, 86%, and 83% of the variations in CH_4 fluxes (Fig. 6), respectively. These coefficient values suggest that ST-25 is the main environmental factor controlling methane emissions from Hongyuan peatland. However, due to the differences in hydrological conditions and plant communities worldwide, this relationship may not generally be applied to other sites. For instance, Rinne et al. (2007) found that the CH_4 fluxes from the Siikaneva Peatland were dependent on soil temperature at -35 cm depth, while Song et al. (2011) confirmed that the variation in soil temperature at −5 cm depth was the best explanation of CH_4 fluxes in a freshwater marsh in the Sanjiang Plain. The results of this study confirm that CH_4 fluxes were significantly correlated with variation in soil temperature, but poorly correlated with air temperature. This indicates that CH_4 emissions from alpine peatland are dominantly controlled by soil temperature. Despite the correlation between changes in CH_4 flux and variation in ST-25 values being calculated as most significant, soil temperature at other depths also exhibited strong correlations with CH_4 flux (Fig. 6). Further research is required to determine the mechanisms that dictate how CH_4 fluxes react to soil temperature change.

4.4. Effects of water table level on ecosystem CH_4 exchange

It is well understood that water table level can play a fundamental role in controlling CH_4 flux from peatlands, by creating aerobic and anaerobic environments within the soil profile (Moore and Roulet, 1993; Treat et al., 2007; Maucieri et al., 2017; Strack and Waddington, 2007). The rate of methanogenesis has been shown to change dramatically with variation in water table level (Shoemaker and Schrag, 2010; Tokida et al., 2007). Numerous researchers have noted that reductions

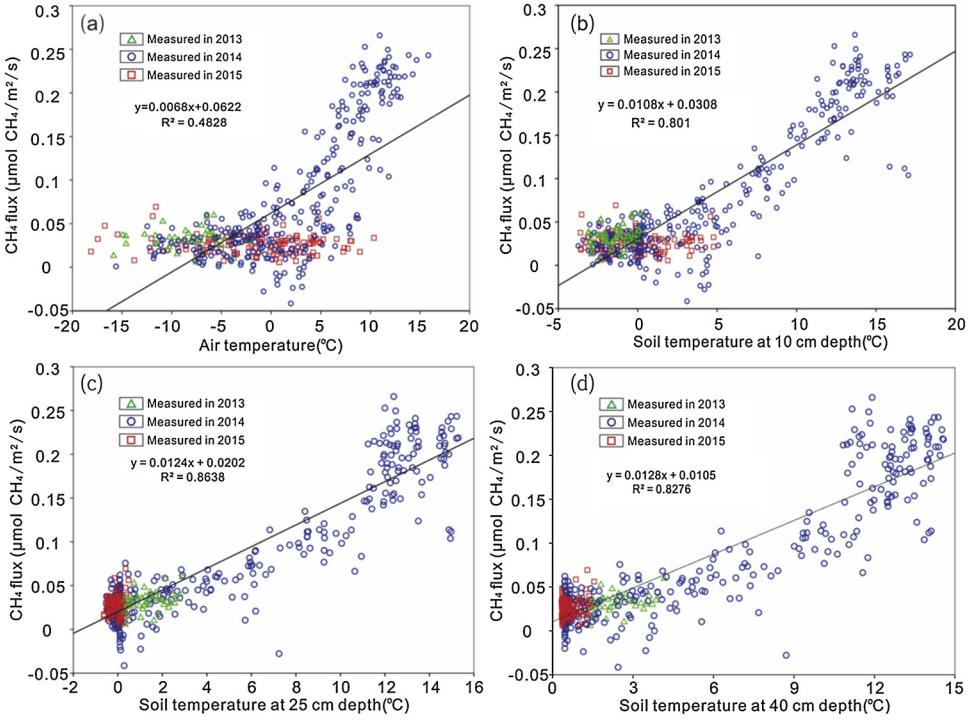

Fig. 6. Dependence of daily mean CH_4 fluxes on: (a) AT200, (b) ST-10, (c) ST-25, and (d) ST-40. Only flux values that have not been gap-filled were used for these correlation analyses.

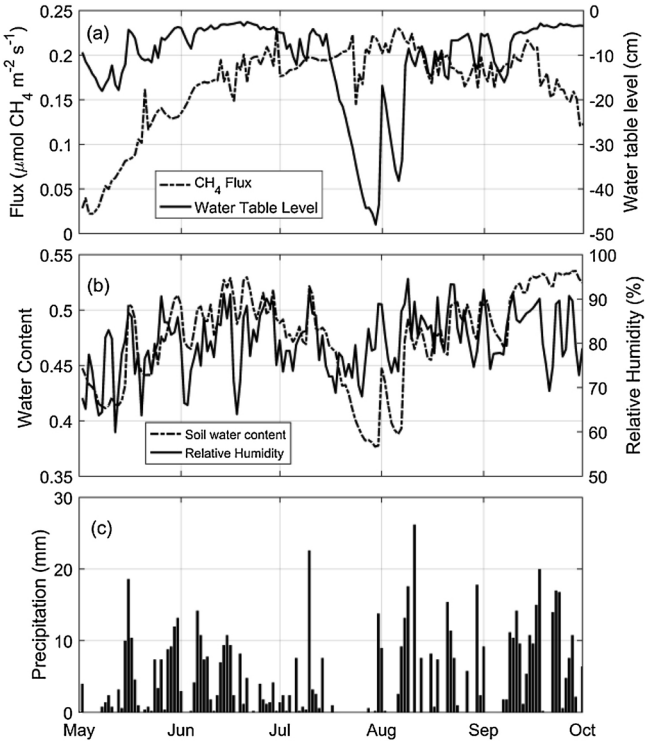

Fig. 7. Time series in growing season: (a) daily mean CH_4 fluxes and water table level; (b) daily mean soil water content and relative air humidity; (c) daily precipitation.

in the level of the water table may lead to a decrease in CH_4 flux (Bridgham et al., 2013; Yang et al., 2014) or drainage (Baldocchi et al., 2012; Urbanová et al., 2013), may lead to a decrease in CH_4 fluxes, while the rewetting and flooding of previously drained peatlands contributes significantly to high CH_4 emissions (Hatala et al., 2012b; Vanselow-Algan et al., 2015). In this study, water table level mostly varied above a depth of -20 cm during the growing season (Fig. 7 a). Therefore, it can be deduced that the anaerobic environment below -20 cm depth was relatively stable for methanogenesis and CH_4 transportation, indicating that CH_4 emissions in the Hongyuan peatland were predominantly derived from a region some 20 cm below the ground surface. This also explains the fact that CH_4 flux was significantly correlated with variations in soil temperature recorded at 25 cm below ground level, where the anaerobic environment is sustained due to inundation (Fig. 6).

Water table depth is an important factor in regulation of the anaerobic conditions required for methanogenesis, and it therefore has a significant influence on CH_4 production (Bubier et al., 1995). Most emitted CH_4 comes from the region below the water table, where the environment is anaerobic due to longtime saturation (Shoemaker et al., 2012). Over the course of this study, abrupt decreases in water table level appeared in late July and early August (Fig. 7a), due to no precipitation in these periods (Fig. 7c). However, only the decrease in water table level in late July caused a small decrease in CH_4 flux, with the decrease in early August having no effect (Fig. 7a). This can be explained by the fact that soil temperatures did not drop in August (Fig. 2c), which appears to have resulted in methanogenesis being unaffected. These results suggest that water table level only controls where CH_4 can be produced, and it is the rate of CH_4 production that is controlled by the soil temperature below the aerobic-anaerobic boundary. Hence, it can be concluded that the aerobic-anaerobic boundary is the key region for CH_4 emission, and the level of the water table and temperature have a synergistic effect on the production of CH_4 emissions.

In this study, no correlation between daily mean CH_4 flux and variation in water table level was observed (Fig. 7a). Hargreaves et al. (2001), Rinne et al. (2007), *and* Song et al. (2011) have previously reported similar observations. Over the period of this study, a drought event caused by low precipitation lasted for 16 days (from day 194 to day 209, in mid-July) during the growing season. During this period, water table level and soil water content decreased simultaneously, but

there was a delay in the decrease in CH_4 flux (Fig. 7). The wavelet analysis results show that the variation in ecosystem CH_4 exchange was not in phase with the variation in water table level on short timescales (Fig. 5h).

5. Conclusions

In this study, *in situ* year-round measurements of CH_4 fluxes were conducted in an alpine peatland on the eastern Qinghai-Tibetan Plateau, from November 2013 to May 2015, using the newly developed LI-7700 open-path CH_4 analyzer. Despite some data gaps owing to technical problems, the gathered data covered all parts of the annual cycle and successfully reflected daily and seasonal variations in CH_4 emissions. Diurnal variation in CH_4 flux was observed during the growing season, with peak flux being recorded at 16:30 daily. Small CH_4 emission surges were observed during the soil thawing and freezing seasons. In addition, using wavelet analysis, the first detailed multi-scale spectral analysis of temporal patterns of alpine peatland CH_4 emission was conducted. The spectral analysis revealed how several variables interact over different timescales, and how their impacts shift during the course of the growing season. Over the study period, the ecosystem was a strong source of CH_4. The intact peatland on the eastern Qinghai-Tibetan Plateau represented a major natural CH_4 source which emitted around 0.15 Tg CH_4 into the atmosphere in 2014, with 75% of this value being emitted during the growing season. The annual variations in CH_4 flux were temperature dependent and specifically depended on the soil temperature at the horizon below the level of the water table. The Q_{10} value of annual CH_4 emission was 5.13, suggesting that the alpine peatland ecosystem would contribute more CH_4 to the global carbon cycle under warming scenarios. The data in this study will aid in quantifying and modeling regional and global CH_4 budgets from alpine peatlands.

Acknowledgments

This research was financially supported by the National Natural Science Foundation of China (grant numbers: 41373134, 41573012, and 41673119), the Strategic Pilot Science and Technology Projects of the Chinese Academy of Sciences (XDA05120501), and the Chinese Academy of Sciences' "Light of West China" Program. Special thanks to the two anonymous reviewers for their valuable comments on the original manuscript.

References

Alberto, M.C.R., et al., 2014. Measuring methane flux from irrigated rice fields by eddy covariance method using open-path gas analyzer. Field Crops Research 160, 12–21.
Aurela, M., Laurila, T., Tuovinen, J.-P., 2002. Annual CO_2 balance of a subarctic fen in northern Europe: Importance of the wintertime efflux. Journal of Geophysical Research: Atmospheres 107 (D21), 4607.
Baldocchi, D., et al., 2012. The challenges of measuring methane fluxes and concentrations over a peatland pasture. Agricultural and Forest Meteorology 153, 177–187.
Baldocchi, D., et al., 2001. FLUXNET: A new tool to study the temporal and spatial variability of ecosystem-scale carbon dioxide, water vapor, and energy flux densities. Bulletin of the American Meteorological Society 82 (11), 2415–2434.
Bousquet, P., et al., 2011. Source attribution of the changes in atmospheric methane for 2006–2008. Atmospheric Chemistry & Physics Discussions 10 (11), 3689–3700.
Bridgham, S.D., Cadillo-Quiroz, H., Keller, J.K., Zhuang, Q., 2013. Methane emissions from wetlands: biogeochemical, microbial, and modeling perspectives from local to global scales. Global Change Biology 19 (5), 1325–1346.
Bubier, J.L., Moore, T.R., Bellisario, L., Comer, N.T., Crill, P.M., 1995. Ecological controls on methane emissions from a Northern Peatland Complex in the zone of discontinuous permafrost, Manitoba, Canada. Global Biogeochemical Cycles 9 (4), 455–470.
Carroll, M.J., Dennis, P., Pearce-Higgins, J.W., Thomas, C.D., 2011. Maintaining northern peatland ecosystems in a changing climate: effects of soil moisture, drainage and drain blocking on craneflies. Global Change Biology 17 (9), 2991–3001.
Cazelles, B., et al., 2008. Wavelet analysis of ecological time series. Oecologia 156 (2), 287–304.
Chai, X., 1981. The formation and types of peat in China and the law of governing its distribution. Acta Geographica Sinica 36, 237–253 (in Chinese with English abstract).
Chen, H., et al., 2013. Inter-Annual Variations of Methane Emission from an Open Fen on the Qinghai-Tibetan Plateau: A Three-Year Study. PloS one 8 (1).
Chen, H., et al., 2010. Diurnal variation of methane emissions from an alpine wetland on the eastern edge of Qinghai-Tibetan Plateau. Environmental Monitoring and Assessment 164 (1-4), 21–28.
Chen, H., et al., 2014. The carbon stock of alpine peatlands on the Qinghai–Tibetan Plateau during the Holocene and their future fate. Quaternary Science Reviews 95 (0), 151–158.
Chen, H., et al., 2008. Determinants influencing seasonal variations of methane emissions from alpine wetlands in Ruoergai Plateau and their implications. Journal of Geophysical Research: Atmospheres 113 (D12) (in Chinese with English abstract).
Conrad, R., 2005. Quantification of methanogenic pathways using stable carbon isotopic signatures: a review and a proposal. Organic Geochemistry 36 (5), 739–752.
Cove, S., et al., 2016. Identifying scale-emergent, nonlinear, asynchronous processes of wetland methane exchange. Journal of Geophysical Research: Biogeosciences 121 (1), 188–204.
Crill, P.M., Martikainen, P.J., Nykǎnen, H., Silvola, J., 1994. Temperature and N fertilization effects on methane oxidation in a drained peatland soil. Soil Biology and Biochemistry 26 (10), 1331–1339.
Cui, M., et al., 2015. Warmer temperature accelerates methane emissions from the Ruoergai wetland on the Tibetan Plateau without changing methanogenic community composition. Scientific Reports 5, 11616.
Dörsch, P., Palojärvi, A., Mommertz, S., 2004. Overwinter greenhouse gas fluxes in two contrasting agricultural habitats. Nutrient cycling in agroecosystems 70 (2), 117–133.
Daubechies, I., 1990. The wavelet transform, time-frequency localization and signal analysis. IEEE Transactions on Information Theory 36 (5), 961–1005.
Deng, Y., Cui, X., Lüke, C., Dumont, M.G., 2013. Aerobic methanotroph diversity in Riganqiao peatlands on the Qinghai–Tibetan Plateau. Environmental Microbiology Reports 5 (4), 566–574.
Detto, M., Verfaillie, J., Anderson, F., Xu, L., Baldocchi, D., 2011. Comparing laser-based open- and closed-path gas analyzers to measure methane fluxes using the eddy covariance method. Agricultural and Forest Meteorology 151 (10), 1312–1324.
Dlugokencky, E.J., Nisbet, E.G., Fisher, R., Lowry, D., 2011. Global atmospheric methane: budget, changes and dangers. Philosophical Transactions of the Royal Society A Mathematical Physical and Engineering Sciences 369 (1943), 2058–2072.
Fletcher, S.E.M., Tans, P.P., Bruhwiler, L.M., Miller, J.B., Heimann, M., 2004. CH 4 sources estimated from atmospheric observations of CH 4 and its 13 C/ 12 C isotopic ratios: 1. Inverse modeling of source processes.
Foken, T., et al., 2005. Post-Field Data Quality Control. In: Lee, X., Massman, W., Law, B. (Eds.), Handbook of Micrometeorology. Atmospheric and Oceanographic Sciences Library. Springer, Netherlands, pp. 181–208.
Franz, D., Koebsch, F., Larmanou, E., Augustin, J., Sachs, T., 2016. High net CO_2 and CH_4 release at a eutrophic shallow lake on a formerly drained fen. Biogeosciences 13 (10), 3051–3070.
Frolking, S., et al., 2011. Peatlands in the Earth's 21st century climate system. Environmental Reviews 19, 371–396.
Fung, I., et al., 1991. Three-dimensional model synthesis of the global methane cycle. Journal of Geophysical Research: Atmospheres 96 (D7), 13033–13065.
Genxu, W., Yuanshou, L., Yibo, W., Qingbo, W., 2008. Effects of permafrost thawing on vegetation and soil carbon pool losses on the Qinghai–Tibet Plateau. China. Geoderma 143 (1–2), 143–152.
Gorham, E., 1991. Northern Peatlands: Role in the Carbon Cycle and Probable Responses to Climatic Warming. Ecological Applications 1 (2), 182–195.
Grinsted, A., Moore, J.C., Jevrejeva, S., 2004. Application of the cross wavelet transform and wavelet coherence to geophysical time series. Nonlinear Processes in Geophysics 11 (5/6), 561–566.
Hargreaves, K., Fowler, D., Pitcairn, C., Aurela, M., 2001. Annual methane emission from Finnish mires estimated from eddy covariance campaign measurements. Theor. Appl. Climatol. 70 (1-4), 203–213.
Hatala, J.A., Detto, M., Baldocchi, D.D., 2012a. Gross ecosystem photosynthesis causes a diurnal pattern in methane emission from rice. Geophys. Res. Lett. 39 (6), L06409.
Hatala, J.A., et al., 2012b. Greenhouse gas (CO_2, CH_4, H_2O) fluxes from drained and flooded agricultural peatlands in the Sacramento-San Joaquin Delta. Agriculture, ecosystems & environment 150, 1–18.
Hendriks, D.M.D., van Huissteden, J., Dolman, A.J., 2010. Multi-technique assessment of spatial and temporal variability of methane fluxes in a peat meadow. Agricultural and Forest Meteorology 150 (6), 757–774.
Heyer, J., Berger, U., Kuzin, I.L., Yakovlev, O.N., 2002. Methane emissions from different ecosystem structures of the subarctic tundra in Western Siberia during midsummer and during the thawing period. Tellus B 54 (3), 231–249.
Hirota, M., et al., 2004. Methane emissions from different vegetation zones in a Qinghai-Tibetan Plateau wetland. Soil Biology and Biochemistry 36 (5), 737–748.
Hong, Y.T., et al., 2005. Inverse phase oscillations between the East Asian and Indian Ocean summer monsoons during the last 12,000 years and paleo-El Niño. Earth and Planetary Science Letters 231 (3–4), 337–346.
Houweling, S., et al., 2017. Global inverse modeling of CH_4 sources and sinks: an overview of methods. Atmos. Chem. Phys. 17 (1), 235–256.
Jin, H.J., Wu, J., Cheng, G.D., Tomoko, N., Sun, G.Y., 1999. Methane emissions from wetlands on the Qinghai-Tibet Plateau. Chinese Science Bulletin 44 (24), 2282–2286.
Jin, Z., Zhuang, Q., He, J.S., Zhu, X., Song, W., 2015. Net exchanges of methane and carbon dioxide on the Qinghai-Tibetan Plateau from 1979 to 2100. Environmental Research Letters 10 (8).
Katul, G., et al., 2001. Multiscale analysis of vegetation surface fluxes: from seconds to years. Advances in Water Resources 24 (9), 1119–1132.
Khalil, M.A.K., Rasmussen, R.A., 1983. Sources, sinks, and seasonal cycles of atmospheric methane. Journal of Geophysical Research: Oceans 88 (C9), 5131–5144.

Kirschke, S., et al., 2013. Three decades of global methane sources and sinks. Nature Geosci 6 (10), 813–823.
Kljun, N., Calanca, P., Rotach, M.W., Schmid, H.P., 2004. A Simple Parameterisation for Flux Footprint Predictions. Boundary-Layer Meteorology 112 (3), 503–523.
Koebsch, F., Jurasinski, G., Koch, M., Hofmann, J., Glatzel, S., 2015. Controls for multi-scale temporal variation in ecosystem methane exchange during the growing season of a permanently inundated fen. Agricultural and Forest Meteorology 204, 94–105.
Koskinen, M., et al., 2014. Measurements of CO2 exchange with an automated chamber system throughout the year: challenges in measuring night-time respiration on porous peat soil. Biogeosciences 11 (2), 347–363.
Lai, D.Y.F., Roulet, N.T., Humphreys, E.R., Moore, T.R., Dalva, M., 2012. The effect of atmospheric turbulence and chamber deployment period on autochamber CO_2 and CH_4 flux measurements in an ombrotrophic peatland. Biogeosciences 9 (8), 3305–3322.
Long, K.D., Flanagan, L.B., Cai, T., 2010. Diurnal and seasonal variation in methane emissions in a northern Canadian peatland measured by eddy covariance. Global Change Biology 16 (9), 2420–2435.
Lund, M., et al., 2010. Variability in exchange of CO_2 across 12 northern peatland and tundra sites. Global Change Biology 16 (9), 2436–2448.
Mastepanov, M., et al., 2008. Large tundra methane burst during onset of freezing. Nature 456 (7222) 628-U58.
Maucieri, C., Barbera, A.C., Vymazal, J., Borin, M., 2017. A review on the main affecting factors of greenhouse gases emission in constructed wetlands. Agricultural and Forest Meteorology 236, 175–193.
McDermitt, D., et al., 2011. A new low-power, open-path instrument for measuring methane flux by eddy covariance. Applied Physics B-Lasers and Optics 102 (2), 391–405.
Meijide, A., et al., 2011. Seasonal trends and environmental controls of methane emissions in a rice paddy field in Northern Italy. Biogeosciences 8 (12), 3809–3821.
Merbold, L., Steinlin, C., Hagedorn, F., 2013. Winter greenhouse gas emissions (CO_2, CH_4 and N_2O) from a sub-alpine grassland. Biogeosciences 10 (1), 3185–3203 10,5(2013-05-13).
Miao, Y., et al., 2012. Growing season methane emission from a boreal peatland in the continuous permafrost zone of Northeast China: effects of active layer depth and vegetation. Biogeosciences 9 (11), 4455–4464.
Moncrieff, J.B., et al., 1997. A system to measure surface fluxes of momentum, sensible heat, water vapour and carbon dioxide. Journal of Hydrology 188, 589–611.
Moore, T.R., Roulet, N.T., 1993. Methane flux: Water table relations in northern wetlands. Geophys. Res. Lett. 20 (7), 587–590.
Morrissey, L.A., Zobel, D.B., Livingston, G.P., 1993. Significance of stomatal control on methane release from Carex-dominated wetlands. Chemosphere 26 (1–4), 339–355.
Mosier, A.R., Bouwman, A.F., 1990. Gas flux measurement techniques with special reference to techniques suitable for measurements over large ecologically uniform areas. Soils and the greenhouse effect.
Papale, D., et al., 2006. Towards a standardized processing of Net Ecosystem Exchange measured with eddy covariance technique: algorithms and uncertainty estimation. Biogeosciences 3 (4), 571–583.
Rinne, J., et al., 2007. Annual cycle of methane emission from a boreal fen measured by the eddy covariance technique. Tellus B 59 (3), 449–457.
Schipper, L.A., Hobbs, J.K., Rutledge, S., Arcus, V.L., 2014. Thermodynamic theory explains the temperature optima of soil microbial processes and high Q10 values at low temperatures. Global Change Biology 20 (11), 3578–3586.
Shoemaker, J.K., Schrag, D.P., 2010. Subsurface characterization of methane production and oxidation from a New Hampshire wetland. Geobiology 8 (3), 234–243.
Shoemaker, J.K., Varner, R.K., Schrag, D.P., 2012. Characterization of subsurface methane production and release over 3 years at a New Hampshire wetland. Geochimica Et Cosmochimica Acta 91, 120–139.
Song, C.C., Sun, L., Huang, Y., Wang, Y.S., Wan, Z.M., 2011. Carbon exchange in a freshwater marsh in the Sanjiang Plain, northeastern China. Agricultural and Forest Meteorology 151 (8), 1131–1138.
Song, W., et al., 2015. Methane emissions from an alpine wetland on the Tibetan Plateau: Neglected but vital contribution of the nongrowing season. Journal of Geophysical Research: Biogeosciences 120 (8) 2015JG003043.
Stocker, T., et al., 2014. IPCC, 2013: climate change 2013: the physical science basis: Contribution of working group I to the fifth assessment report of the intergovernmental panel on climate change. Cambridge University Press, New York.
Strack, M., Waddington, J., 2007. Response of peatland carbon dioxide and methane fluxes to a water table drawdown experiment. Global Biogeochemical Cycles 21 (1).
Thauer, R.K., Kaster, A.-K., Seedorf, H., Buckel, W., Hedderich, R., 2008. Methanogenic archaea: ecologically relevant differences in energy conservation. Nature Reviews Microbiology 6 (8), 579–591.
Thomas, E.K., et al., 2014. Abundant C_4 plants on the Tibetan Plateau during the Lateglacial and early Holocene. Quaternary Science Reviews 87, 24–33.
Thomas, K.L., Benstead, J., Davies, K.L., Lloyd, D., 1996. Role of wetland plants in the diurnal control of CH_4 and CO_2 fluxes in peat. Soil Biology and Biochemistry 28 (1), 17–23.
Tokida, T., et al., 2007. Episodic release of methane bubbles from peatland during spring thaw. Chemosphere 70 (2), 165–171.
Torrence, C., Compo, G.P., 1998. A Practical Guide to Wavelet Analysis. Bulletin of the American Meteorological Society 79 (1), 61–78.
Treat, C.C., Bubier, J.L., Varner, R.K., Crill, P.M., 2007. Timescale dependence of environmental and plant-mediated controls on CH4 flux in a temperate fen. Journal of Geophysical Research: Biogeosciences (G01014), 112.
Tseng, K.-H., et al., 2010. Determination of methane and carbon dioxide fluxes during the rice maturity period in Taiwan by combining profile and eddy covariance measurements. Agricultural and Forest Meteorology 150 (6), 852–859.
Turunen, J., Tomppo, E., Tolonen, K., Reinikainen, A., 2002. Estimating carbon accumulation rates of undrained mires in Finland - application to boreal and subarctic regions. Holocene 12 (1), 69–80.
Urbanová, Z., Bárta, J., Picek, T., 2013. Methane Emissions and Methanogenic Archaea on Pristine, Drained and Restored Mountain Peatlands, Central Europe. Ecosystems 16 (4), 664–677.
Van Dijk, A., Moene, A., De Bruin, H., 2004. The principles of surface flux physics: theory, practice and description of the ECPACK library. Meteorology and Air Quality Group, Wageningen University, Wageningen, The Netherlands 99 pp.
Vanselow-Algan, M., et al., 2015. High methane emissions dominated annual greenhouse gas balances 30 years after bog rewetting. Biogeosciences 12 (14), 4361–4371.
Vargas, R., Allen, M.F., 2008. Environmental controls and the influence of vegetation type, fine roots and rhizomorphs on diel and seasonal variation in soil respiration. New Phytologist 179 (2), 460–471.
Vickers, D., Mahrt, L., 1997. Quality control and flux sampling problems for tower and aircraft data. Journal of Atmospheric and Oceanic Technology 14 (3), 512–526.
Walter, B.P., Heimann, M., Matthews, E., 2001. Modeling modern methane emissions from natural wetlands: 1. Model description and results. Journal of Geophysical Research: Atmospheres 106 (D24), 34189–34206.
Wang, D., et al., 2002. Methane emission from marshes in Ruoergai Plateau. Advance in Earth Sciences 17 (6), 876–880 (in Chinese with English abstract).
Webb, E., Pearman, G., Leuning, R., 1980. Correction of flux measurements for density effects due to heat and water vapour transfer. Quarterly Journal of the Royal Meteorological Society 106 (447), 85–100.
Wei, D., et al., 2015. Revisiting the role of CH_4 emissions from alpine wetlands on the Tibetan Plateau: Evidence from two in situ measurements at 4758 and 4320 m above sea level. Journal of Geophysical Research: Biogeosciences 120 (9), 1741–1750.
WMO/GAW, 2017. WMO GREENHOUSE GAS Bulletin: The State of Greenhouse Gases in the Atmosphere Based on Global Observations through 2016. World Meteorological Organization, Geneva.
Xiang, S., Guo, R., Wu, N., Sun, S., 2009. Current status and future prospects of Ruoergai Marsh in Eastern Qinghai-Tibet Plateau. Ecological Engineering 35 (4), 553–562.
Yang, G., et al., 2014. Effects of soil warming, rainfall reduction and water table level on CH_4 emissions from the Ruoergai peatland in China. Soil Biology and Biochemistry 78, 83–89.
Yao, L., Zhao, Y., Gao, S., Sun, J., Li, F., 2011. The peatland area change in past 20 years in the Ruoergai Basin, eastern Tibetan Plateau. Frontiers of Earth Science 5 (3), 271.
Ye, R., Keller, J.K., Jin, Q., Bohannan, B.J.M., Bridgham, S.D., 2014. Mechanisms for the suppression of methane production in peatland soils by a humic substance analog. Biogeosciences Discuss. 2014, 1739–1771.
Yu, Z.C., Loisel, J., Brosseau, D.P., Beilman, D.W., Hunt, S.J., 2010. Global peatland dynamics since the Last Glacial Maximum. Geophys. Res. Lett. 37 (13), 69–73.
Yuan, Q., Pump, J., Conrad, R., 2012. Partitioning of CH_4 and CO_2 Production Originating from Rice Straw, Soil and Root Organic Carbon in Rice Microcosms. PloS one 7 (11).
Yvon-Durocher, G., et al., 2014. Methane fluxes show consistent temperature dependence across microbial to ecosystem scales. Nature 507 (7493), 488–491.
Zhang, B., et al., 2017. Methane emissions from global wetlands: An assessment of the uncertainty associated with various wetland extent data sets. Atmospheric Environment 165, 310–321.
Zhu, D., Chen, H., Wu, N., Wang, Y., Luo, P., 2011. Winter methane emission from an alpine open fen on Tibetan Plateau. Polish Journal of Ecology 59 (1), 87–94.